IEEE Access
Multidisciplinary | Rapid Review | Open Access Journal

Received October 29, 2020, accepted November 14, 2020, date of publication November 18, 2020,
date of current version December 3, 2020.

Digital Object Identifier 10.1109/ACCESS.2020.3038857

Embryonics Based Phased Array Antenna Structure With Self-Repair Ability

SAI ZHU, CHUNHUI HAN, YAFENG MENG, JIAWEN XU, AND TING AN
Department of Electronic and Optical Engineering, Army Engineering University, Shijiazhuang Campus, Shijiazhuang 050003, China

Corresponding authors: Sai Zhu (szhumail@163.com) and Chunhui Han (cartoonhch@163.com)

This work was supported by the National Natural Science Foundation of China under Grant 61601495, and the Youth Talent Promotion Project for Military Science and Technology under Grant 18-JCJQ-QT-001.

ABSTRACT The reliability of phased array antenna can be improved with the self-repairing technology, and the existing self-repair method based on the TR module reconfiguration has problems such as slow calculation speed and difficulty in calculating the elements' mutual coupling, which is difficult to meet the application requirements. In this paper, a novel phased array antenna structure with self-repair ability is proposed. Based on the embryological electronics (embryonics), a novel phased array antenna structure with TR cell as the basic unit is constructed. The faulty TR cell can be detected and removed, and its influence on the phased array antenna's performance can be eliminated. The function and connection of faulty TR cell can be implemented by the normal TR cells and idle TR cells, the performance of phased array antenna can be repaired in real-time. TR cell, TR cell array and input/output switching control module are designed. The simulation tests show that, the phased array antenna with various fault conditions can be repaired in real-time based on the proposed structure, and the performance of phased array antenna can be repaired to the initial normal state with enough idle TR cells in array. Even without the idle TR cell, the performance of phased array antenna with fault can be improved through the self-repair. A new way for the design of phased array antenna design with self-repair ability is provided.

INDEX TERMS Embryonics, faulty cell elimination, phased array antenna, self-repair, TR cell.

I. INTRODUCTION

Phased array antenna is widely used in modern radar equipment due to its high power, high gain, and fast beam scanning. Phased array antenna is composed of a large number of TR modules and elements, and the amplitude and phase of each element's signal can be changed through TR module. The high-power, high-gain, and differently directed beams can be synthesized. A large number of TR modules are the basis of the phased array antenna. As the increase of the TR module's number, the probability of phased array antenna failure is increased. The phased array antenna's performance could be declined with the TR module's failure [1], [2], which seriously affects its intended design function. At the same time, the phased array antenna is complicated, and its faulty components are difficult to be repaired. Especially in the aerospace, battlefield and other application environments, the fault cannot be repaired in time.

The associate editor coordinating the review of this manuscript and approving it for publication was Debdeep Sarkar.

When the fault occurred on several modules among numerous TR modules in phased array antenna, the remaining normal TR module in phased array antenna could be reconfigured with self-repair and correction technology [3], [4], and phased array antenna's performance could be corrected and repaired [5], [6].

In the current research, when the fault is identified, the excitation and its control code [7] of remaining elements [8] or compensation sub-array [9] is recalculated. The corresponding TR modules are reconfigured to minimize the difference between the original pattern and the repaired pattern in presence of faults [10], [11]. Therefore, researchers have paid great attention to the excitation recalculation, and different calculating methods have been studied. Some intelligence optimization algorithm based schemes have been reported, including genetic algorithms (GA) [7], [12]–[14], adaptive genetic algorithm (AGA) [15], firefly algorithm (FA) [12], [16], [17], particle swarm optimization (PSO) [10], [18], quantum particle swarm optimization (QPSO) [19], bacteria foraging optimization

(BFO) [10], cuckoo search algorithm [20], cuckoo search–chicken swarm optimization (CSCSO) [21], flower pollination algorithm [22], [23], recursive intelligent optimizer (RIO) [24], whale optimization algorithm (WOA) and chaotic whale optimization algorithm (CWOA) [25], grey wolf optimizer hybridized with an interior point algorithm [26], greedy sparseness constrained optimization (GSCO) technique [27], differential evolution (DE) algorithm [28], Taguchi algorithm [29]. Iterative Fourier transform (IFT) [5], [30], [31] and quantized IFT (QIFT) [32] is another method for calculating the excitation of remaining elements. Besides the calculation methods based on intelligence optimization algorithm and IFT, there are other techniques based error minimization scheme, such as cumulative sum (CUSUM) [11], matrix pencil technique (MPT) [33]–[35], conjugate symmetry approach[36], minimum norm least-square [37]. After the excitation was calculated, the remaining TR modules would be reconfigured to obtain the repaired pattern which is similar to the original pattern. During the pattern's correction and repair based on the TR module reconfiguration, the excitation of each element was changed during reconfiguration, and the mutual coupling between elements would be changed [38]–[40]. And the phased array antenna actual repaired pattern would be different from the theory pattern [41], so that the actual repair effect would be affected.

Inspired by the embryonic electronic system, a novel phased array antenna structure with self-repair ability is proposed. The TR module is re-designed as TR cell, and the phased array antenna is re-built with TR cell. The repair control circuit in the novel phased array antenna is researched, and the proposed self-repair structure provides a new method for the phased array antenna's design.

The rest of this paper is organized as follows. In Section II, the background of phased array antenna self-repair and embryonics are introduced. In Section III, the proposed self-repair structure is presented in detail, and the phased array antenna's self-repair process based on the proposed structure is analyzed in Section IV. The simulation tests are realized, and the proposed phased array antenna structure's self-repair ability is verified and analyzed in Section V. Finally, conclusions are reached in Section VI. Furthermore, more suggestions are put forward for future research.

II. PHASED ARRAY ANTENNA SELF-REPAIR AND EMBRYONICS

A. PHASED ARRAY ANTENNA'S BASIC STRUCTURE AND SELF-REPAIR

A typical phased array antenna structure is given in FIGURE 1, which is composed of element array, TR module array, beam control system, and power distribution/addition network [11], [42]. The phase and amplitude of each transceiving channel's signal can be configured and the radiation beam can be controlled.

In the existing phased array antenna self-repair study, the normal element's excitation is modified through adjusting the control code of phase shifter and attenuator in TR module.

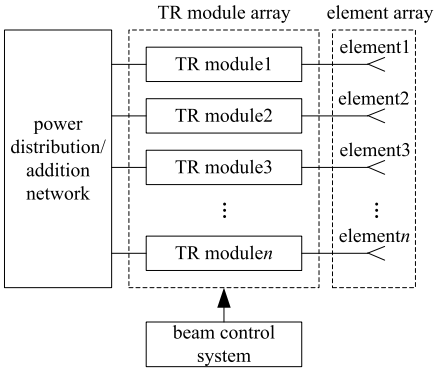

FIGURE 1. Phased array antenna basic structure.

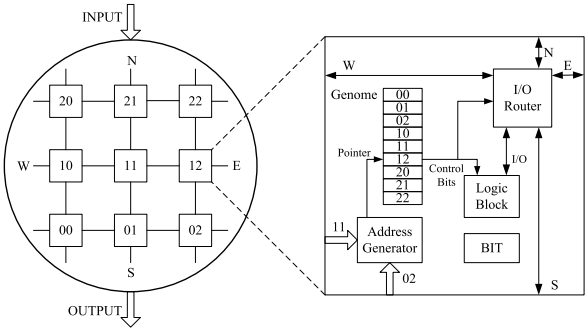

FIGURE 2. The basic structure of embryonics.

The phased array antenna's pattern is corrected to reduce the fault's impact on the beam based on the excitation reconfiguration. The phased array antenna's performance can be restored to the maximum extent, and the self-repair of phased array antenna is achieved.

Aiming at the normal beam pattern, the control code of normal TR modules' phase shifter and attenuator is calculated through the group intelligence algorithm, iterative FFT and matrix beam method. Those optimization-based algorithms are time-consuming due to blind-search features, which simply perform heuristic operators that improve solutions iteration-by-iteration. Besides, each element's excitation is changed during the self-repair process, and mutual coupling between different elements is changed as well. The self-repair result is affected by the changing mutual coupling, and it is difficult to obtain the theoretical calculation results. Thus, repair needs are hardly to be satisfied in practice.

B. EMBRYONICS

The embryological electronics (embryonics) is a bionic hardware structure with self-detection and self-repair ability, and it is composed of electronic cells with the same structure, which is illustrated in FIGURE 2 [43].

The electronic cell is a logical unit with processing capabilities. The cell's expressed gene can be specialized according to its position, and its logic function and I/O unit's connection is determined. When a cell is faulty, its fault signal can be transmitted, and the self-repair is triggered. The faulty

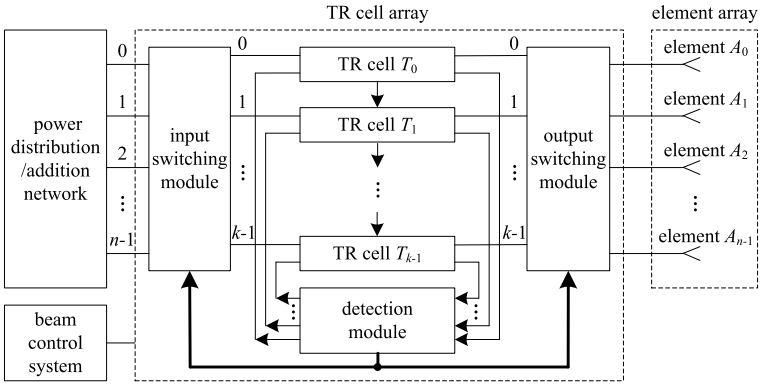

FIGURE 3. Phased array antenna self-repair structure based on embryonics.

cell would be removed to eliminate the fault's influence. The remaining cells recalculate the location and update the expressed genes to perform a new function and connection. Through the faulty cells' removal and the normal cells' replacement [44], the target circuit function is maintained, and the self-repair is completed based on embryonics.

III. PHASED ARRAY ANTENNA SELF-REPAIR STRUCTURE BASED ON EMBRYONICS

A. PHASED ARRAY ANTENNA SELF-REPAIR STRUCTURE

Based on the embryonics, the phased array antenna is redesigned as given in FIGURE 3. The proposed phased array antenna's structure is composed of element array, TR cell array, power distribution/addition network and beam control system. The TR cell array is composed of k TR cells $(T_0, T_1, \ldots, T_{k-1})$, detection module, input switching module and output switching module.

The RF signal's transmission, reception and the adjustment of phase and amplitude can be realized by TR cell. A cell chain is constituted with all the k TR cells, where $k \geq n$, and k-n is the number of backup TR cells, that is, the number of failures that would be repaired. In the normal state, the first n TR cells $(T_0, T_1, \ldots, T_{n-1})$ are working cells, and the signal transmission, reception and adjustment of n elements $(A_0, A_1, \ldots, A_{n-1})$ in phased array antenna is performed with the n working TR cells. The last k-n TR cells $(T_n, T_{n+1}, \ldots, T_{k-1})$ are backup cells. When a working cell is faulty, the function of the faulty cell and its following cells are sequentially shifted, and the latter cell realizes the function of the previous cell until using a backup cell.

The detection module detects the TR cells' state in real-time, and generates a fault signal according to the detected result. The TR cell's state, input switching module and output switching module are controlled by the fault signal.

The connection between the power distribution/addition network and TR cell is accomplished with input switching module, under the control of the detection module's result. Only the working TR cells are connected to the power distribution/addition network, and the faulty TR cells would be disconnected from the power distribution/addition network.

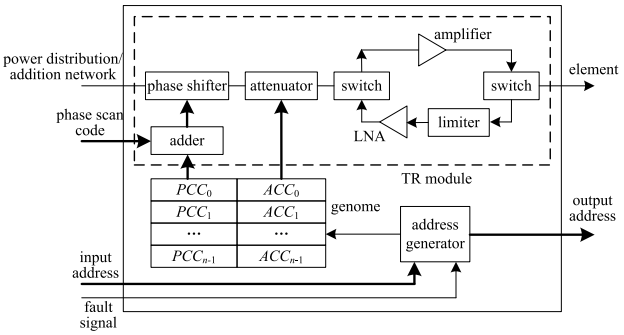

FIGURE 4. TR cell structure.

The output switching module's function is similar to the input switching module. The connection between n working TR cells and n elements is accomplished with the output switching module. Only the working TR cell would be connected to elements, and the elements' normal signal can be kept.

B. TR CELL STRUCTURE

All TR cells have the same structure, which is composed of TR module, genome and address generator, as detailed in FIGURE 4.

The TR module is composed of controllable attenuator, controllable phase shifter, transmit amplifier, receive limiter, low noise amplifier (LNA), switch and adder. One port of the TR module is connected to the power distribution/addition network, and the other port is connected to the element. The signal power can be amplified and limited, and its phase and amplitude can be adjusted with different phase shifter control codes and attenuator control codes. The phase shifter control code from the genome and the phase scan code are added with an adder, and the summation is used to configure the controllable phase shifter. The beam's scanning can be realized under different phase scan codes.

All the n genes of the entire phased array antenna are stored in genome. Each gene is composed of a phase control code $(PCC_i,\ i = 0, 1, \ldots, n-1)$ and an attenuator control code $(ACC_i, i\ = 0, 1, \ldots, n-1)$, and the phase shifter and the

attenuator in the TR module are controlled respectively. The TR module's function can be configured with the different genes, and the signal's phase and amplitude can be adjusted. Each cell in the TR cell array performs different genes, so that the amplitude and phase of different elements' transceiving signals are distributed according to a certain rule, constructing the expected beam pattern. For the phased array antenna with a larger scale, the number of genes in each TR cell is larger due to the numerous elements. The integration memory can be used to store the genome, and the programmable logic controller can be used to the gene's writing and reading.

The TR cell's address signal A_{do} can be generated with address generate module according to the input address A_{di} and fault signal F, and the cell's expressed gene can be selected with the address signal. The relationship between A_{di}, F, and A_{do} is shown in (1)

$$A_{do} = A_{di} + \bar{F} \tag{1}$$

That is, when TR cell is normal, its fault signal $F = 0$, the cell address is the input address plus 1; when the cell is faulty, its fault signal $F = 1$, the cell address is equal to its input address.

The input address signal and output address signal of adjacent TR cells are connected to each other, forming a cell chain with all TR cells. The different genes can be selected and expressed by each cell according to the cell's state signal F and address signal A_{do}. Each TR cell's address signal is increased sequentially in the cell chain, and its expressed gene in the genome is sequentially increased too. When a TR cell is faulty, its output address signal is equal to the input address signal, and the following cell would have the same address as the faulty TR cell's original address and expressed the faulty TR cell's expressed gene.

There are three states (working, faulty and idle) for a TR cell. The working cell is the normal cell performing attenuation and phase shifting, and it is connected to the power distribution/addition network and element one by one. The faulty cells are the cells that have been failed, and cannot perform the function of attenuation and phase shifting. The faulty cell would be no longer connected to the power distribution/addition network and the element. The idle cell is the normal TR cell in backup state. When the working cell is failed, the idle cell could turn to be working cell, which ensures the number of working cells in the system to be n, and maintain the phased array antenna function.

C. INPUT/OUTPUT SWITCHING MODULE

The number of elements and the power distribution/addition network's port is n, and the number of TR cells is k, where $k > n$. There are n working cells and its position changes continuously when the fault occurred.

The connection between working cells with the power distribution/addition network and element is realized by the input/output switching module. When a working cell is failed, its connection to the power distribution/addition network and element would be cut off in time, and the connection of the cells after the faulty cell would be updated, until an idle cell turned to be the working cell, and connected to the power distribution/addition network and element. The faulty cell's disconnection, the working cell's update and the idle cell's connection is realized by the input switching module and output switching module.

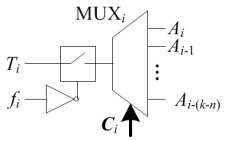

FIGURE 5. The structure of TR cell's output switching module.

The input switching module's structure is as same as the output switching module. Taking the output switching module as an example, it performs switching control between k TR cells $T_0, T_1, \ldots, T_{k-1}$ and n elements $A_0, A_1, \ldots, A_{n-1}$, according to the TR cells' fault signal. The n working cells are always connected to the corresponding n elements with the output switching module. For the understanding easily, suppose there are k-n virtual elements $A_n, A_{n+1}, \ldots, A_{k-1}$ in phased array antenna, and all virtual array elements are empty port, then the number of TR cells is equal to the elements' number.

Considering the connection between TR cell T_i and the element, the following conditions exist:

(1) In the initial state, all the TR cells are normal, then its fault signal $f_j = 0, j = 0, 1, \ldots, k-1$, and the TR cell T_i would be connected to element A_i;
(2) When the TR cell T_i is faulty, its fault signal $f_i = 1$, and the connection between TR cell T_i and element would be cut off;
(3) When the TR cell T_i is normal, and the cell before T_i is faulty, then $f_i = 0, f_j = 1, j \in \{0, 1, \ldots, i-1\}$. The TR cell T_i would be connected to the element before A_i, and the serial number of the connecting element is $i - \sum_{j=0}^{i-1} f_j$.

Combining the three connection cases above, the connection of T_i can be expressed as

$$T_i = \bar{f}_i A_{i-\sum_{j=0}^{i-1} f_j} \tag{2}$$

To realize the function shown in (2), a multiplexer (MUX) and a switch are used to connect T_i with $k - n$ elements $A_i, A_{i-1}, \ldots, A_{i-(k-n)}$, and the connection is shown in FIGURE 5.

In the TR cell's output switching module illustrated in FIGURE 5, the connections between TR cell T_i and elements $A_i, A_{i-1}, \ldots, A_{i-(k-n)}$ are controlled by the fault signal f_i of T_i. When T_i is normal, $f_i = 0$, the NOT gate's output is 1, and the switch is closed. And the TR cell T_i would be connected to an element through the multiplexer MUX$_i$; When T_i is failed, $f_i = 1$, the NOT gate's output is 0 and the switch is cut off. And the TR cell T_i would be disconnected to any element.

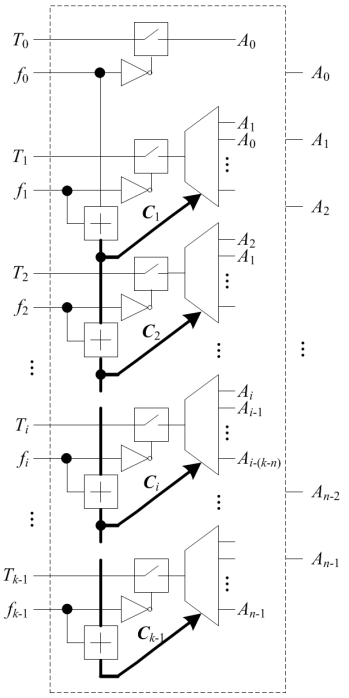

FIGURE 6. The structure of TR cell array's output switching module.

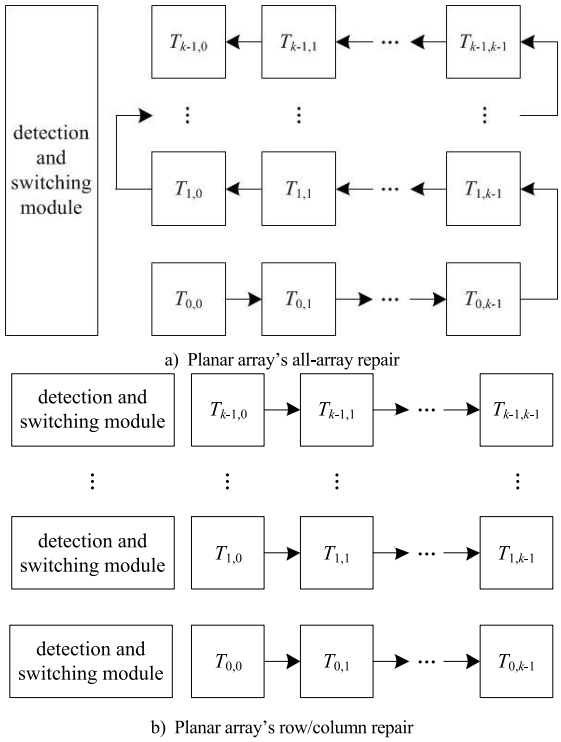

FIGURE 7. Planar array's self-repair. The $T_{i,j}$ is the TR cell addressed in ith cow and jth column in planar array. The detection and switching module is the same as the detection module, the input switching module and the output switching module in FIGURE 3.

The multiplexer MUX_i controls the connection between T_i with $A_i, A_{i-1}, \ldots, A_{i-(k-n)}$, and its control signal C_i is

$$C_i = \sum_{j=0}^{i-1} f_i \tag{3}$$

In the TR cell's output switching module shown in FIGURE 5, the number of multiplexer's port is $\geq k-n+1$, so the width of the multiplexer's control signal C_i is

$$width(C_i) = \lceil \log_2(k-n+1) \rceil \tag{4}$$

where $width(C_i)$ represents the width of the signal C_i, $\lceil \bullet \rceil$ is the ceiling function. The first $k-n+1$ ports of the multiplexer are connected to the corresponding elements, and the subsequent ports are blanked.

For all TR cells in the phased array antenna, its output switching module is designed as FIGURE 5, where $i = 1, 2, \ldots, k-1$. And the virtual element and the element with the sequence number $i-(k-n) < 0$ are set to be blank. The structure of the TR cell array's output switching module is detailed as FIGURE 6.

The output switching module shown in FIGURE 6 is composed of k switches, k NOT gates, $k-1$ adders, and k multiplexers. For the TR cell T_0, it is connected to only one element A_0, and its other connected element's sequence number is $0-(k-n) < 0$, which means that it is empty and should be set to be blank. So no multiplexer is used, the TR cell T_0 is directly connected to element A_0 through a switch. For the TR cells T_i whose sequence number is $i > n-1$, if its connected element's sequence number is greater than $n-1$, the connecting element is a virtual element. And the multiplexer's port that is connected to a virtual element should be set to empty in the output switching module shown in FIGURE 6.

The width of the adder's output in FIGURE 6 is the same as the width of the multiplexer's control signal, and it is $\lceil \log_2(k-n+1) \rceil$.

IV. SELF-REPAIR PROCESS

A. PHASED ARRAY ANTENNA'S SELF-REPAIR

The proposed self-repair structure can be used for the self-repair of both linear array and planar array. When the proposed structure is employed for the linear array's self-repair, the linear array can be designed as FIGURE 3 with TR cells, and a TR cell chain can be composed of all the TR cells in the linear array. The faulty TR cell in the chain can be eliminated, and the linear array can be repaired.

When the planar array is designed with the proposed structure, there would be a TR cell chain or several TR cell chains existing in the planar array. The faulty TR cell can be removed and replaced with the idle TR cells in the chain or chains, and the planar array self-repair could be accomplished. According to the number of TR cell chains, the planar array's self-repair can be divided as all-array repair and row/column repair. Taking the rectangle planar array as an example, its all-array repair and row/column repair is indicated in FIGURE 7.

In the all-array repair, the rectangle planar array is composed of TR cell array, detection and switching module, as shown in FIGURE 7 a). And only a TR cell chain existed in the rectangle planar array, which is composed of all the

TR cells. The idle TR cells existed in the TR chain, and it can be used to repair any faulty TR cell in the planar array. In row/column repair, the rectangle planar array is composed of TR cell array, several detection and switching modules, as indicated in FIGURE 7 b). There are sever TR cell chains that existed in the rectangle planar array, and each TR cell chain is composed of the TR cells in the same row/column. There are a corresponding detection and switching module for each TR cell chain, and the idle cells existed in each TR cell chain, which can be used to repair the fault in the corresponding row/column. And the self-repair can be accomplished with the corresponding detection and switching module.

B. SELF-REPAIR PROCESS

In the initial state, the first n TR cells are connected to the power distribution/addition network and the elements, and different genes are expressed by each TR cell according to its position. During phased array antenna working, each TR cell's state is detected by the detection module in real-time.

When a TR cell is failed, its fault signal is set to be high by the detection module. Driven by the fault signal, the functions of the faulty TR cell and its following cells are sequentially shifted until an idle TR cell is used, so that the working cells' number is maintained as n. At the same time, the connections of the input switching module and the output switching module are changed based on the TR cells' fault signals. The connections between the faulty TR cell with the power distribution/addition network and element are cut off, and the used idle TR cell is connected to the corresponding power distribution/addition network and element. The state of the element signal could be maintained and the phased array antenna can be repaired.

Taking the phased array antenna with 3 elements and 5 TR cells as an example, $n = 3, k = 5$. Its normal state and repair process is indicated in FIGURE 8. The gene in the genome with boldface is the TR cell's expressed gene.

The initial phased array antenna is shown in FIGURE 8 a). In the initial state, the output of the T_0 address generator is 0, and the gene0, gene1 and gene2 are expressed by T_0, T_1, and T_2 correspondingly, which are connected to the element A_0, A_1 and A_2. T_3 and T_4 are the idle cells and connected to non-element.

When T_1 is faulty, it is disconnected to the element A_1, and the address generate module of T_1 output 0, which is as same as T_0. Then T_2's address is equal to the T_1's original address, which is 1. The gene1 and gene2 are expressed by T_2 and T_3 correspondingly, which are connected to A_1 and A_2. The T_4 is still an idle cell. When the self-repair process is finished, the genes gene0, gene1, gene2 are expressed by normal TR cells T_0, T_2, T_3, which are connected to the elements A_0, A_1, A_2. So the signals of elements A_0, A_1, A_2 would be kept as normal, and the phased array antenna has been repaired, as shown in FIGURE 8 b).

During the self-repair process, the expressed genes of the TR cells after faulty TR cell are changed according to the address, and the functions and connections of the faulty TR cell and the following TR cells are shifted to the next neighbor TR cell, until the idle TR cell is used. The function and connection of the faulty TR cell would be implemented by a normal TR cell. Each element is connected to normal TR cell with the proper function as the initial state, and the self-repair could be achieved.

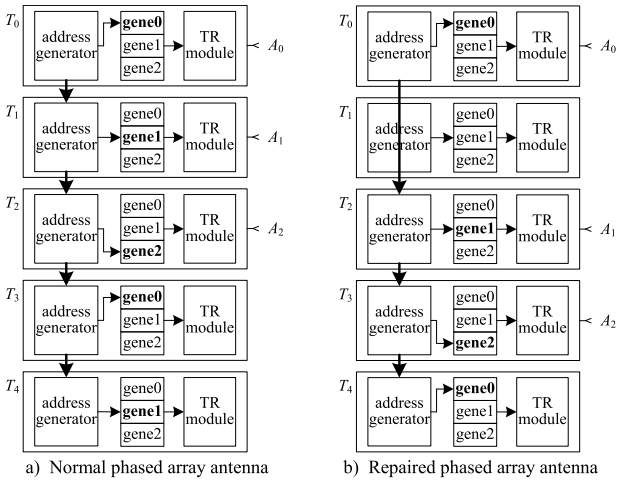

FIGURE 8. Self-repair process of phased array antenna. The location of elements A_0, A_1, A_2 is fixed, and the connections between the TR cells and antennas were changed during self-repair.

The updating of TR cells' function and connection is realized with a combinational circuit, and all the TR cells after the faulty TR cell would be updated at the same time. And the phased array antenna's repair would be accomplished as soon as the faulty TR cell is detected.

In this adjacent neighbor TR cell replaced method, each TR cell is connected to $k - n$ elements with the switch and detection module. The switch scale is determined by the idle TR cells' number, and not be influenced by the phased array antenna's scale. So the self-repair's complex could be reduced with the proposed updating method, and self-repair of the phased array antenna with a larger scale could be realized.

V. SIMULATION TEST

Taking the self-repair of a linear phased array antenna with 16 elements as an example, the proposed self-repair structure is simulated and tested. The phased array antenna is constructed with 16 elements, 16 working TR cells and 6 idle TR cells, based on the proposed structure. The 22 TR cells are numbered as TRC_0, TRC_1, …, TRC_21, and the 16 elements are noted as Antenna_0, Antenna_1, …, Antenna_15.

The phased array antenna's repair control circuit is implemented in the Xilinx ISE 12.2, and the repair process is simulated using the simulation software ISim of ISE. The phased array antenna's pattern and the parameters such as maximum sidelobe level, average sidelobe level, half-power lobe width are calculated with Matlab, according to each TR cell's phase control code and attenuator control code got in Xilinx ISE simulation. And the self-repair result is analyzed

TABLE 1. Element's normalized excitation.

j	I_j	j	I_j
0	0.1138	8	1.0000
1	0.1964	9	0.9353
2	0.3319	10	0.8163
3	0.4926	11	0.6613
4	0.6613	12	0.4926
5	0.8163	13	0.3319
6	0.9353	14	0.1964
7	1.0000	15	0.1138

TABLE 2. Element's attenuator control code, attenuation and actual normalized excitation.

j	AC_j	AS_j (dB)	I_j
0	100110	19.0	0.1122
1	011100	14.0	0.1995
2	010011	9.5	0.3350
3	001100	6.0	0.5012
4	000111	3.5	0.6683
5	000100	2.0	0.7943
6	000001	0.5	0.9441
7	000000	0.0	1.0000
8	000000	0.0	1.0000
9	000001	0.5	0.9441
10	000100	2.0	0.7943
11	000111	3.5	0.6683
12	001100	6.0	0.5012
13	010011	9.5	0.3350
14	011100	14.0	0.1995
15	100110	19.0	0.1122

based on the pattern and parameters of the repaired phased array antenna.

In the simulation experiment, different TR cell fault situations such as single TR cell fault, adjacent multiple TR cells fault, and multiple TR cells sequence fault are analyzed.

A. PHASED ARRAY ANTENNA STATE AND SIMULATION SETUP

The element spacing is set as 0.5λ (λ is the wavelength of the radiated electromagnetic wave), and each element is numbered as $0, 1, \ldots, 15$, respectively. The Dolph-Chebyshev amplitude weighted synthesis is used, and the normalized excitation I_j of the element j is shown in TABLE 1.

In the TR cell, a 6-bit digital attenuator is used to control the amplitude of the element's signal. The control codes of attenuator range from 000000 to 111111, and the corresponding attenuation is from 0dB to 31.5dB, 0.5dB as the interval. The attenuator control code for element j is noted as AC_j, and its attenuation is AS_j. AC_j, AS_j, and actual normalized excitation I_j are shown in TABLE 2.

Only the Dolph-Chebyshev amplitude weighting is used, and phase weighting is not used in the simulation. So each phase shifter's control code is 000000 (The 6-bit digital phase shifter is used in TR cell). The genes of 21 TR cells are shown in TABLE 3.

In TABLE 3, the TR cells from TRC_16 to TRC_21 are idle cells, and their genes are 000000000000.

Under the configuration shown in TABLE 3, the pattern of linear phased array antenna is shown in FIGURE 9.

TABLE 3. Gene of each TR cell.

i	TRC_i	i	TRC_i
0	000000 100110	11	000000 000111
1	000000 011100	12	000000 001100
2	000000 010011	13	000000 010011
3	000000 001100	14	000000 011100
4	000000 000111	15	000000 100110
5	000000 000100	16	000000 000000
6	000000 000001	17	000000 000000
7	000000 000000	18	000000 000000
8	000000 000000	19	000000 000000
9	000000 000001	20	000000 000000
10	000000 000100	21	000000 000000

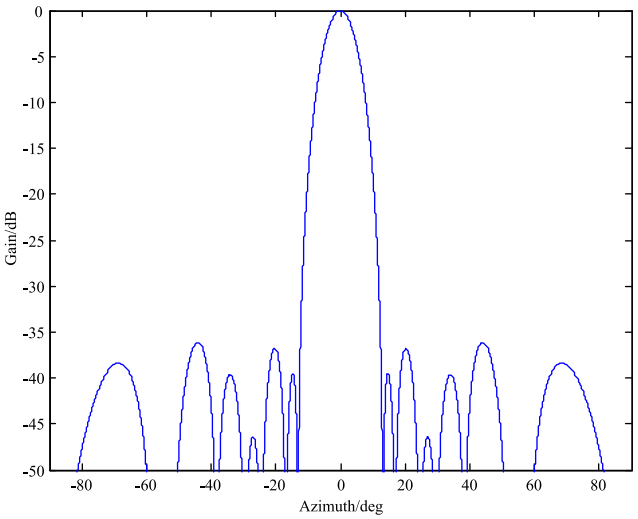

FIGURE 9. Pattern of the linear phased array antenna in normal state.

TABLE 4. Parameters of the linear phased array antenna in normal state.

Parameter	maxSLL (dB)	avSLL (dB)	HPBW (deg)	FNBW (deg)
Value	-36.12	-41.21	8.93	26.33

The pattern's maximum sidelobe level (maxSLL), the average sidelobe level (avSLL), half power lobe width (HPBW) and first null lobe width (FNBW) are shown in TABLE 4.

In the simulation, $k = 22$, $n = 16$, the number of multiplexer's ports in the output switching module is $\geq k - n + 1 = 7$, so the 1-8 multiplexer is selected, and the width of its control signal is $\lceil \log_2(k - n + 1) \rceil = 3$.

To test the proposed phased array antenna's self-repair process, the TR cell's fault signal f_i is set manually to provide a startup signal for the repair process. The self-repair ability of the proposed phased array antenna's structure is verified through the changing of TR cell's state, expressed gene, element's attenuator control code in the self-repair process, and it is confirmed through pattern calculation.

B. SINGLE TR CELL FAULT SELF-REPAIR

The TR cell TRC_4 is set to be faulty, and the signal of the connected element Antenna_4 is turned to be 0. The pattern of the linear phased array antenna with the fault is shown as FIGURE 10, and its parameters are given in TABLE 5.

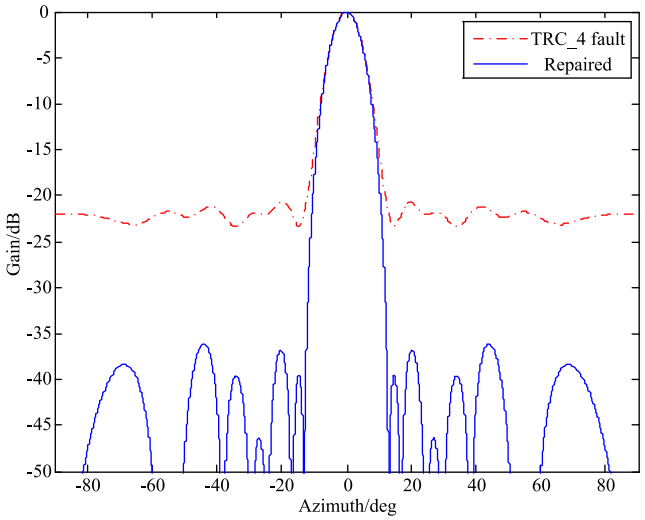

FIGURE 10. Pattern of the linear phased array antenna with TRC_4 fault and repaired.

TABLE 5. Parameters of the linear phased array antenna with TRC_4 Fault and Repaired.

Parameter		maxSLL (dB)	avSLL (dB)	HPBW (deg)	FNBW (deg)
Value	TRC_4 fault	-20.69	-21.50	9.07	29.65
	Repaired	-36.12	-41.21	8.93	26.33

In can be found from FIGURE 10 and TABLE 5 that, the phased array antenna's pattern is distorted greatly as TRC_4 fault. The maximum sidelobe level is raised from −36.12dB to −20.69dB, and the average sidelobe level is increased from −41.21 dB to −21.50 dB. Both the half power lobe width and the first null lobe width are widened.

As soon as the fault occurred, the self-repair was started, and the TR cells' function and the connection were adjusted. The self-repair process is shown in FIGURE 11.

In FIGURE 11, TRC_i_AtConf($i = 0, 1, \ldots, 21$) is the attenuator control code outputted by ith TR cell. F_i is the fault signal of the ith TR cell. Antenna_j_AtConf($j = 0, 1, \ldots, 15$) is the attenuator control code of the TR cell connected to the jth element, and it is the control code of the attenuator through which the element radiates the signal.

At 200ns, the TR cell TRC_4 is faulty, and its fault signal is set to be high, F4 = 1. The addresses of TRC_4 and following TR cells are changed, and their express genes are changed as well. The functions of the faulty TR cell and the TR cells after are shifted in sequence. The TRC_5_AtConf is the TRC_4's original output 000111. And the TRC_6_AtConf is the TRC_5's original output 000100, ...until the idle TR cell TRC_16 is used, and TRC_16_AtConf is the TRC_15's original output 100110.

Driven by the fault signal, the connection between TR cells and elements is updated. And the all the elements connected to the TR cell that implemented the original connected TR cell's function, ensuring the function of each element remains unchanged.

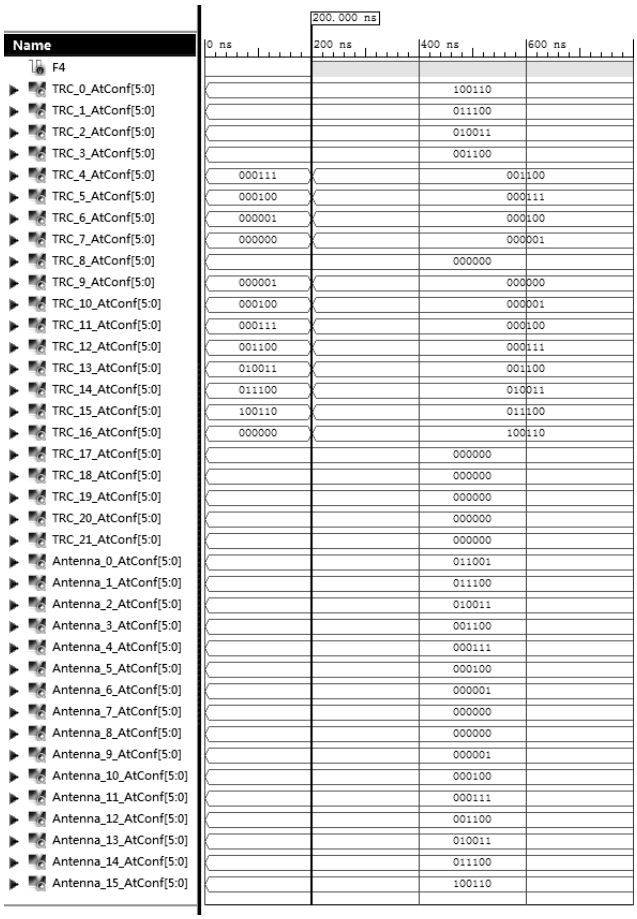

FIGURE 11. Self-repair process of single TR cell fault.

TABLE 6. Parameters of the linear phased array antenna with TRC_7, TRC_8 fault.

Parameter		maxSLL (dB)	avSLL (dB)	HPBW (deg)	FNBW (deg)
Value	TRC_7, TRC_8 fault	-11.27	-13.42	7.78	17.84
	Repaired	-36.12	-41.21	8.93	26.33

As soon as the faulty TR cell TRC_4's fault signal is high, at 200ns, the repair process is completed, under the control of address generator and detection module, which is a combinational circuit. The repaired phased array antenna's pattern is shown in FIGURE 10 and its parameters are shown in TABLE 5. The repaired pattern is corrected as same as the initial pattern shown in FIGURE 9, the parameters are also equal to the values shown in TABLE 4. The phased array Antenna with single TR cell fault is repaired successfully, and its pattern is repaired to the initial normal state.

C. ADJACENT MULTIPLE TR CELLS SIMULTANEOUS FAULT SELF-REPAIR

The adjacent TR cells TRC_7 and TRC_8 are faulty at the same time, and the radiation signals of the elements Antenna_7 and Antenna_8 are 0. The pattern of phased array antenna with faulty TR cells is given in FIGURE 12. And its parameters are shown in TABLE 6.

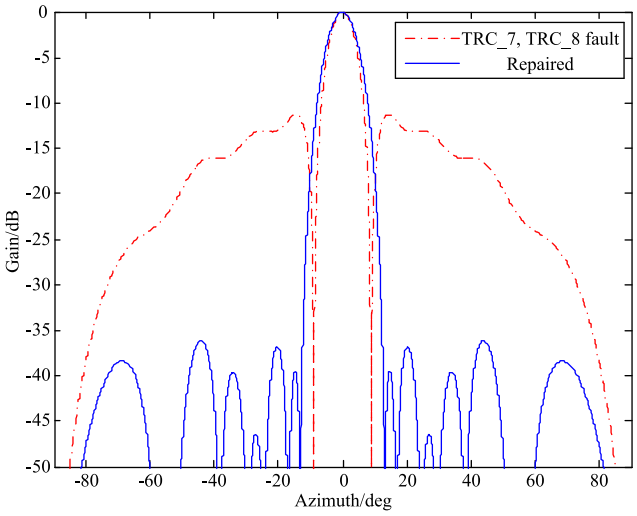

FIGURE 12. Pattern of phased array antenna with TRC_7, TRC_8 fault.

It can be seen from FIGURE 12, TABLE 6 that, the pattern of the phased array antenna with TRC_7, TRC_8 fault is severely distorted, and its maxSLL and avSLL are raised to −11.27dB, −13.42dB respectively.

The self-repair process is shown in FIGURE 13. At 200 ns, the two adjacent TR cells TRC_7 and TRC_8 are failed simultaneously, and their fault signals are high at the same time, that is, F7 = 1, F8 = 1. Driven by the fault signal, the expressed genes and functions of the faulty TR cells and the following TR cells are shifted one by one, until the two idle TR cells TRC_16, TRC_17 are used. The TRC_*i*_AtConf (i = 9, 10, …, 17) are changed. TRC_9_AtConf is TRC_7's original output 000000, TRC_10_AtConf is TRC_8's original output 000000, …., and TRC_17_AtConf is the TRC_15's original output 100110. Under the control of the output switching module, the connection between TR cells and elements is updated.

At 200ns, the repair is completed. Through the shifting of TR cells function and connection, each element's configured attenuator control code is kept unchanged. The repaired phased array antenna's pattern and its parameters are shown in FIGURE 12 and TABLE 6. The phased array antenna with adjacent multiple faulty TR cells is repaired absolutely, and its pattern is precisely recovered to the initial pattern.

D. MULTIPLE TR CELL SEQUENCE FAULT SELF-REPAIR

When multiple TR cells are failed sequence, the self-repair process is shown in FIGURE 14.

At 200ns, TRC_6 is failed, and its fault signal is set to be high, F6 = 1. At 300ns, TRC_9 and TRC_11 are failed simultaneously, F9 = 1, F11 = 1. At 400ns, TRC_0 is failed, F0 = 1. At 500ns TRC_15 and TRC_16 are failed simultaneously, F15 = 1 and F16 = 1. At 600 ns, TRC_2 is failed, F2 = 1.

When the cells failed at 200ns, 300ns, 400ns and 500ns, the functions of cells following the faulty TR cells are sequentially shifted, and the elements' connected TR cells

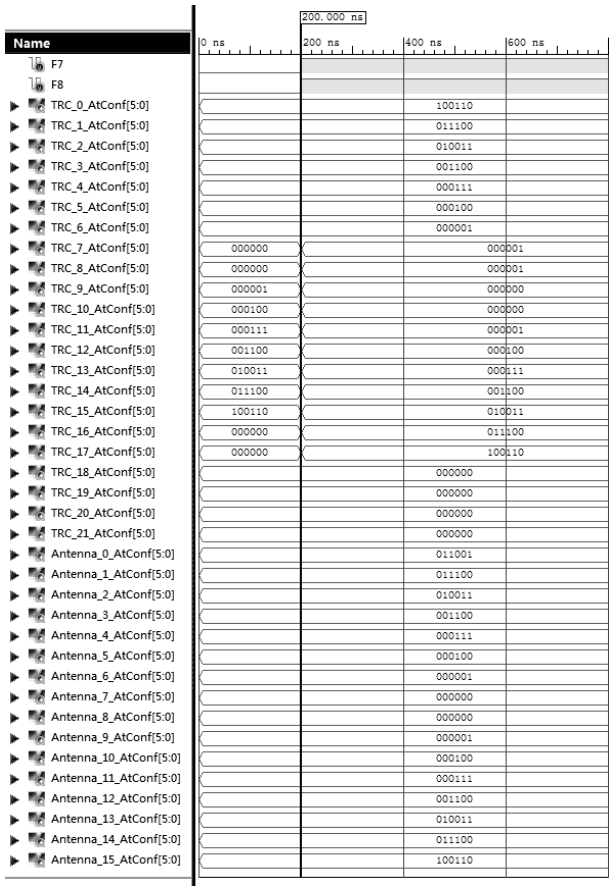

FIGURE 13. Self-repair process of phased array antenna with TRC_7, TRC_8 fault.

TABLE 7. Parameters of phased array antenna with TRC_2 fault and repair under no idle TR cell.

Parameter		maxSLL (dB)	avSLL (dB)	HPBW (degree)	FNBW (degree)
Value	TRC_2 fault	-29.20	-31.09	9.24	26.42
	Repaired under no idle TR cell	-32.61	-35.88	9.16	25.73

are changed under the control of the output switching module. The elements are always connected to the normal TR cells, and their configured attenuator control code remains unchanged. The phased array antenna's pattern is repaired as normal shown in FIGURE 9.

At 600ns, when TRC_2 is faulty, the pattern of phased array antenna is shown in FIGURE 15, and its parameters are given in TABLE 7.

Comparing the pattern with TRC_2 fault to the normal pattern in FIGURE 15, we can find that the pattern is distorted, and its parameters are degraded.

As soon as the TRC_2's fault signal is set to be high, the self-repair is started under the control of the address generator and detection module, which is a combinational circuit. The functions and connection of TRC_2 and the following cells are shifted in sequence according to the self-repair rule. At 600ns, the cumulative number of faulty TR cells in the phased array antenna is 7, which is bigger than the number of

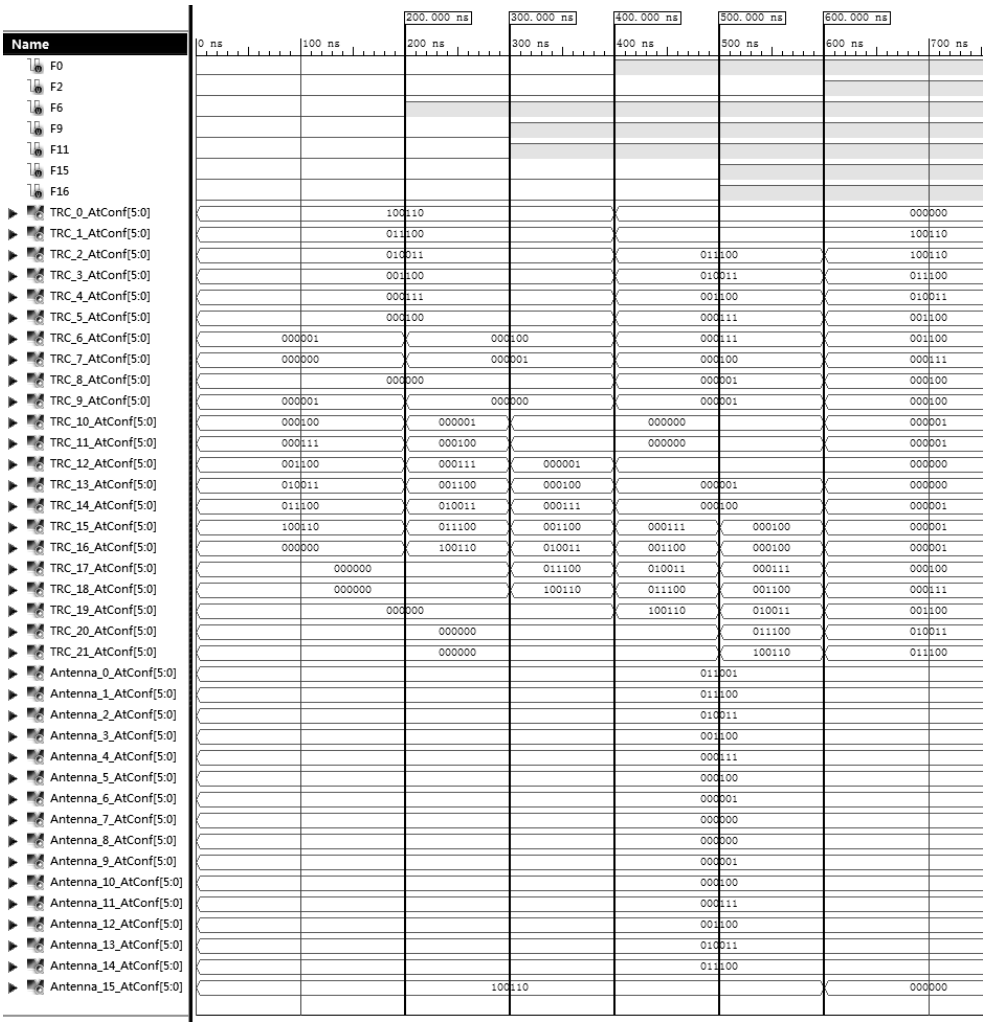

FIGURE 14. Self-repair process of phased array antenna with multiple TR cell sequence fault.

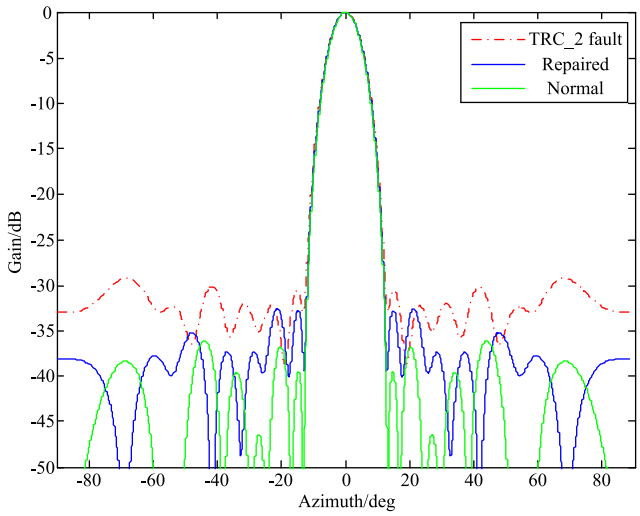

FIGURE 15. Pattern of phased array antenna with TRC_2 fault and repaired under no idle TR cell.

idle TR cells. Therefore the phased array antenna has no more backup TR cells. The element Antenna_14 is connected to the last normal TR cell TRC_21, and Antenna_15 cannot be connected to any normal TR cell. And the phased array antenna cannot be repaired to the initial normal state. Although the simulation result shows that Antenna_15_AtConf is 000000, there is no input RF signal for Antenna_15 due to the lack of normal TR cell, and its excitation signal is 0. At this time, the attenuator control code Antenna_j_AtConf, the attenuation AS_j, and the normalized excitation I_j for each element are shown in TABLE 8.

With the configuration of TABLE 8, the repaired phased array antenna's pattern is shown in FIGURE 15. And its parameters are shown in TABLE 7.

It can be seen from FIGURE 15 and TABLE 7, the pattern and performance of the phased array antenna with faulty TRC_2 is improved through self-repair. The repaired pattern is less than perfect as the initial normal pattern, but it has been corrected to be better than the faulty pattern. Its maxSLL has descended from −29.20dB to −32.61dB, the avSLL has descended from −31.09dB to −35.88dB, the HPBW and the FNBW are changed from 9.24 degree, 26.42 degree to 9.16 degree, 25.73 degree respectively. As there is not enough

TABLE 8. Attenuator control code, attenuation and normalized excitation of each element after self-repair.

j	AC_j	AS_j (dB)	I_j
0	100110	19.0	0.1122
1	011100	14.0	0.1995
2	010011	9.5	0.3350
3	001100	6.0	0.5012
4	000111	3.5	0.6683
5	000100	2.0	0.7943
6	000001	0.5	0.9441
7	000000	0.0	1.0000
8	000000	0.0	1.0000
9	000001	0.5	0.9441
10	000100	2.0	0.7943
11	000111	3.5	0.6683
12	001100	6.0	0.5012
13	010011	9.5	0.3350
14	011100	14.0	0.1995
15	-	-	0

backup TR cell in the array, the phased array antenna is not repaired to the initial normal state, but has been improved from the faulty pattern.

E. COMPARE WITH THE EXISTING TECHNOLOGY

The phased array antenna with 32 elements is analyzed and compared under the existing technology [10] and the proposed method. When its sixth and ninth elements are failed, its reconfiguration excitations are calculated with the bacteria foraging optimization (BFO).

The phased array antenna is analyzed in HFSS 15.0. 32 rectangular microstrip patch antennas are applied to construct a linear array. The radiation signal frequency is 2.45GHz, and the inter-element spacing is $\lambda/2$. During the simulation, the source is set according to the reconfiguration excitations in [10]. And the ideal recovered pattern and the recovered pattern with mutual coupling are analyzed with the same excitation. And the normal pattern, ideal recovered pattern without mutual coupling and the recovered pattern with mutual coupling are shown in FIGURE 16.

From FIGURE 16 we can see that, the ideal recovered pattern without mutual coupling is closed to the normal pattern, and the maximum sidelobe level is closed to the original in theory. But influenced by the mutual coupling, the actual repaired pattern is distorted. The actual sidelobe level is higher than the ideal, and the repair effect is reduced.

The phased array antenna is realized with the proposed self-repair structure. When the sixth and ninth TR cells are failed, the faulty TR cells can be moved away from the array, and the idle TR cells are used. The faulty TR cells' function is implemented by the normal cells and each element is connected to the normal working TR cell. When the repair process is finished, the signal of each element is as same as the initial, so the repaired pattern with the proposed structure and the initial normal pattern are identical as shown in FIGURE 16. The repair effect is improved with the proposed phased array antenna structure.

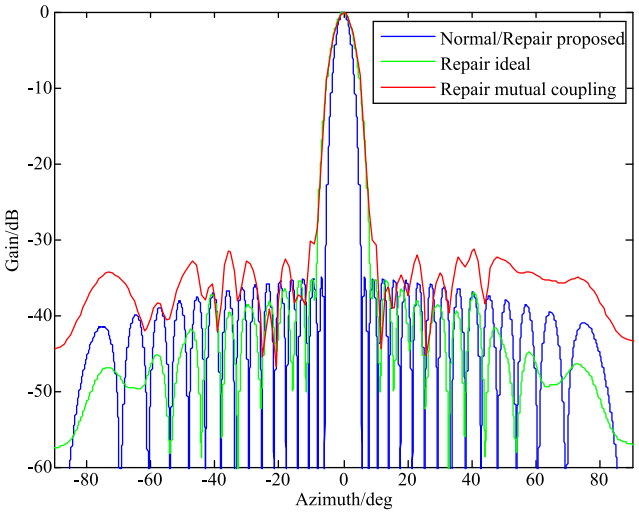

FIGURE 16. Normal pattern, ideal repaired pattern and the repaired pattern with mutual coupling.

F. ANALYSIS FOR SELF-REPAIR RESULT

The self-repair simulation, including single TR cell fault, adjacent multi-TR cell fault, and multi-TR cell sequence fault, demonstrate that, the self-repair process of the proposed phased array antenna structure can be completed under different fault conditions.

In the self-repair process, the functions and connections of TR cells are changed, and the radiation signal of each element is kept to be unchanged, which makes the coupling between the elements of the repaired phased array antenna is as same as initial.

During the proposed phased array antenna's self-repair, the TR cells' expressed gene and connection are controlled by the address generator and detection module, which is a combinational circuit. And the function and connection of all TR cells in the proposed structure would be updated at the same time in the self-repair process as the simulation test shown. The computation time would not be increased with phased array antenna's size changing. But in the simulation test, the self-repair process is analyzed with ideal switches, and the switching time was not considered. The self-repair time would be increased in practical, and it is influenced by the switching speed of switches, which is about at the level of microsecond (μs).

The simulation in this paper is finished under the ideal condition, and the phase shifter and attenuator of different TR cells are kept to be uniform. But the actual phase shifter and attenuator used in phased array antenna cannot be completely consistent, and there is a deviation between different phase shifters and attenuators. Although the deviation can be reduced by the compensation of each TR cell, it cannot be eliminated thoroughly. So the actual self-repair effect of the proposed phased array antenna structure would deviate from the ideal result as the simulation test shown in this paper, and the deviation is determined by the degree of inconsistency between different phase shifters and attenuators of different

TR cells. The actual repair effect of the proposed phased array antenna structure would be analyzed and studied by constructing an experimental system in the next research.

The self-repair capability of the proposed structure is determined by the number of idle TR cells, and it would be higher as the backup TR cells' number increased. At the same time, the system complexity would be increased along with the number of idle cells. So the number of idle cells could be optimized according to the system self-repair capability and complexity. For the phased array antenna with a larger scale, the gene number in each TR cell would be big. Since the gene is short in length, the genome scale would not be too larger to be stored, and it can be satisfied with the integration memory and program logic controller. Take the phased array antenna with 100000 elements as an example, if 8-bit digital phase shifter and 8-bit digital attenuator are used. The scale of the genome would be $100000 \times (8+8) = 1600000$bit, and it can be satisfied with a 128K$\times$16bit integration memory. The proposed system can be employed for the phased array antenna with a larger scale. At the same time, dividing the phased array antenna with larger-scale into small scale array, and configuring idle cells for each sub-array is another solution to reducing the idle TR cells' number and the genome scale.

VI. CONCLUSION AND NEXT WORK

Inspired by the embryonics, a novel phased array antenna structure with self-repair ability is proposed, and a new technical approach for phased array antenna's repair is provided. The phased array antenna self-repair structure proposed in this paper has the following characteristics:

(1) Based on the proposed structure, the real-time self-repair can be realized through the fast switching of TR cells, and phased array antenna's self-repair speed has been improved. After the repair process is completed, each element's radiation signal of the repaired phased array antenna is the same as the initial normal state. The mutual coupling between the elements is kept to be consistent as the initial state, and the influence of the changing mutual coupling on the repair result has been avoided, and the self-repair effect has been improved.

(2) The self-repair of the proposed structure is accomplished through the faulty TR cells' replacement with idle TR cells, and the self-repair capability is limited by the idle TR cell number. In practical applications, the idle TR cell number can be configured according to the TR cell number, element number and the phased array antenna's self-repair requirement.

(3) With the advancement of technology, the integration of TR module has been improved, and its area has been reduced, providing a foundation for the integration design of TR cell. At the same time, the element array's area is fixed by the elements' number, the elements' spacing, and the frequency of the radiation signal. The integrated design of TR cells provides the foundation that a certain number of idle TR cells can be configured in the same space of element array.

(4) The proposed structure is composed of digital control circuit and the RF circuit. The power distribution/addition network, input/output switching module, and elements are included in the RF circuit, and lots of RF switches are used in the proposed structure to achieving the self-repair. So the application scope is limited by the RF switch. Now the frequency of commercial FR switch ranges from hundreds MHz to hundreds GHz, and the targeted frequency of operation is the same as the commercial FR switch, and the mmWave system is supported with the proposed structure.

In this paper, only the digital circuit such as the genome, address generator of the TR cell and the output switching module, are simulated in the experiments, and the TR cell's TR module and element's radiated signal are calculated by Matlab. In the follow-up study, the TR cell hardware would be built, and the phased array antenna experiment system would be constructed based on the proposed structure, and the self-repair ability of the proposed phased array antenna structure would be verified and evaluated. The repair result of the reconfiguration method and the proposed method would be compared and analyzed, and the mutual coupling influence would be analyzed. In the future studies, the number of idle TR cell for large scale phased array antenna would be analyzed, the influence of practical switches, phase shifters and attenuators would be studied. And the real-time testing measurement of phased array antenna would be researched.

REFERENCES

[1] T. He, G. Zhu, and L. Wang, "Possible fault types and impact analysis of phased array antennas," in *Proc. IEEE 4th Adv. Inf. Technol., Electron. Autom. Control Conf. (IAEAC)*, Chengdu, China, Dec. 2019, pp. 1612–1615.

[2] S. Vakalis and J. A. Nanzer, "Analysis of element failures in active incoherent microwave imaging arrays using noise signals," *IEEE Microwave Wireless Compon. Lett.*, vol. 29, no. 2, pp. 161–163, Feb. 2019.

[3] K. M. Lee, R. S. Chu, and S. C. Liu, "A built-in performance-monitoring/fault isolation and correction (PM/FIC) system for active phased-array antennas," *IEEE Trans. Antennas Propag.*, vol. 41, no. 11, pp. 206–209, Nov. 1993.

[4] Q. Lingling, J. Tao, Q. Jiahui, and Y. Yuqi, "Evaluation of failed arrays pattern recovery based on genetic algorithm," in *Proc. Int. Appl. Comput. Electromagn. Soc. Symp.-China (ACES)*, Beijing, China, Jul. 2018, pp. 1–3.

[5] W. P. M. N. Keizer, "Element failure correction for a large monopulse phased array antenna with active amplitude weighting," *IEEE Trans. Antennas Propag.*, vol. 55, no. 8, pp. 2211–2218, Aug. 2007.

[6] B. Tang, J. Zhou, B. Tang, Y. Wang, and L. Kang, "Adaptive correction for radiation patterns of deformed phased array antenna," *IEEE Access*, vol. 8, pp. 5416–5427, Jan. 2020.

[7] H.-T. Chou and D.-Y. Cheng, "Beam-pattern calibration in a realistic system of phased-array antennas via the implementation of a genetic algorithm with a measurement system," *IEEE Trans. Antennas Propag.*, vol. 65, no. 2, pp. 593–601, Feb. 2017.

[8] X. G. Zhang, W. X. Jiang, H. W. Tian, Z. X. Wang, Q. Wang, and T. J. Cui, "Pattern-reconfigurable planar array antenna characterized by digital coding method," *IEEE Trans. Antennas Propag.*, vol. 68, no. 2, pp. 1170–1175, Feb. 2020, doi: 10.1109/TAP.2019.2938678.

[9] S. I. Gusev and O. V. Spirkina, "The efficiency of spatial preprocessor in case of antenna array element failure," in *Proc. 6th Medit. Conf. Embedded Comput. (MECO)*, Bar, Montenegro, Jun. 2017, pp. 1–4.

[10] O. P. Acharya and A. Patnaik, "Antenna array failure correction," *IEEE Antennas Propag. Mag.*, vol. 59, no. 6, pp. 106–115, Jun. 2017.
[11] Y.-S. Chen and I.-L. Tsai, "Detection and correction of element failures using a cumulative sum scheme for active phased arrays," *IEEE Access*, vol. 6, pp. 8797–8809, Mar. 2018.
[12] X. Jiang, J. Qin, and T. Jiang, "Comparing the failure correction ability between GA and FA for array antenna," in *Proc. Joint Int. Symp. Electromagn. Compat., Sapporo Asia–Pacific Int. Symp. Electromagn. Compat. (EMC Sapporo/APEMC)*, Sapporo, Japan, Jun. 2019, pp. 737–740.
[13] X. Jiang, P. Xu, and T. Jiang, "Comparison between NU-CNLMS and GA for antenna array failure correction," in *Proc. IEEE Int. Symp. Antennas Propag. USNC/URSI Nat. Radio Sci. Meeting*, Boston, MA, USA, Jul. 2018, pp. 2205–2206.
[14] J.-H. Han, S.-H. Lim, and N.-H. Myung, "Array antenna TRM failure compensation using adaptively weighted beam pattern mask based on genetic algorithm," *IEEE Antennas Wireless Propag. Lett.*, vol. 11, pp. 18–21, Mar. 2012.
[15] J. Miao, X. Zhang, Q. Chen, and Y. Chen, "Antenna array pattern correction with failure elements using AGA," in *Proc. Int. Appl. Comput. Electromagn. Soc. Symp. (ACES)*, Suzhou, China, Aug. 2017, pp. 1–3.
[16] N. S. Grewal, M. Rattan, and M. S. Patterh, "A non-uniform circular antenna array failure correction using firefly algorithm," *Wireless Pers. Commun.*, vol. 97, no. 1, pp. 845–858, May 2017.
[17] H. Patidar, G. K. Mahanti, and R. Muralidharan, "Synthesis and failure correction of flattop and cosecant squared beam patterns in linear antenna arrays," *J. Telecommun. Inf. Technol.*, vol. 4, pp. 25–30, Jan. 2018.
[18] A. M. Engroff, L. A. Greda, M. P. Magalhaes, A. Winterstein, L. S. Pereira, A. G. Girardi, and M. V. T. Heckler, "Comparison of beamforming algorithms for retro-directive arrays with faulty elements," in *Proc. 10th Eur. Conf. Antennas Propag. (EuCAP)*, Davos, Switzerland, Apr. 2016, pp. 1–5.
[19] L. Poli, A. Massa, P. Rocca, and G. Oliveri, "Failure correction in time-modulated linear arrays," *IET Radar, Sonar Navigat.*, vol. 8, no. 3, pp. 195–201, Mar. 2014.
[20] R. Muralidharan, A. Vallavaraj, G. K. Mahanti, and H. Patidar, "QPSO for failure correction of linear array of mutually coupled parallel dipole antennas with desired side lobe level and return loss," *J. King Saud Univ.-Eng. Sci.*, vol. 29, no. 2, pp. 112–117, Apr. 2017.
[21] R. Muralidaran, A. Vallavaraj, H. Patidar, and G. K. Mahanti, "Failure correction of linear array of antenna with multiple null placement using cuckoo search algorithm," *ICTACT J. Commun. Technol.*, vol. 5, no. 1, pp. 877–881, Jan. 2014.
[22] S. Liang, T. Feng, and G. Sun, "Sidelobe-level suppression for linear and circular antenna arrays via the cuckoo search–chicken swarm optimisation algorithm," *IET Microwave, Antennas Propag.*, vol. 11, no. 2, pp. 209–218, Jan. 2017.
[23] S. Evsdsnslk, M. V. Krishna, and G. Raju, "Pattern recovery in linear array antenna using flower pollination algorithm," in *Proc. IEEE Int. Conf. Intell. Syst. Green Technol. (ICISGT)*, Visakhapatnam, India, Jun. 2019, pp. 53–56.
[24] H. Patidar and G. K. Mahanti, "Failure correction of linear antenna array by changing length and spacing of failed elements," *Prog. Electromagn. Res. M*, vol. 61, pp. 75–84, Oct. 2017.
[25] Z. Hamici, "Fast beamforming with fault tolerance in massive phased arrays using intelligent learning control," *IEEE Trans. Antennas Propag.*, vol. 67, no. 7, pp. 4517–4527, Jul. 2019.
[26] P. Patel, G. Kumari, and P. Saxena, "Array pattern correction in presence of antenna failures using Metaheuristic optimization algorithms," in *Proc. Int. Conf. Commun. Signal Process. (ICCSP)*, Chennai, India, Apr. 2019, pp. 695–700.
[27] S. U. Khan, M. K. A. Rahim, and L. Ali, "Correction of array failure using grey wolf optimizer hybridized with an interior point algorithm," *Frontiers Inf. Technol. Electron. Eng.*, vol. 19, no. 9, pp. 1191–1202, Sep. 2018.
[28] S. U. Khan, M. K. Rahim, M. Aminu-Baba, and M. A. Murad, "Correction of failure in linear antenna arrays with greedy sparseness constrained optimization technique," *PLoS ONE*, vol. 12, no. 12, pp. 1–18, Dec. 2017.
[29] S. K. Mandal, S. Patra, S. Salam, K. Mandal, G. K. Mahanti, and N. N. Pathak, "Failure correction of linear antenna arrays with optimized element position using differential evolution," in *Proc. IEEE Annu. India Conf. (INDICON)*, Bengaluru, India, Dec. 2016, pp. 1–5.
[30] K. Yadav, A. K. Rajak, and H. Singh, "Array failure correction with placement of wide nulls in the radiation pattern of a linear array antenna using iterative fast Fourier transform," in *Proc. IEEE Int. Conf. Comput. Intell. Commun. Technol.*, Ghaziabad, India, Feb. 2015, pp. 471–474.
[31] W. P. M. N. Keizer, "Low-sidelobe pattern synthesis using iterative Fourier techniques coded in MATLAB [EM programmer's notebook]," *IEEE Antennas Propag. Mag.*, vol. 51, no. 2, pp. 137–150, Apr. 2009.
[32] W. P. M. N. Keizer, "Low sidelobe phased array pattern synthesis with compensation for errors due to quantized tapering," *IEEE Trans. Antennas Propag.*, vol. 59, no. 12, pp. 4520–4524, Dec. 2011.
[33] H. Shen and B. Wang, "An effective method for synthesizing multiple-pattern linear arrays with a reduced number of antenna elements," *IEEE Trans. Antennas Propag.*, vol. 65, no. 5, pp. 2358–2366, May 2017.
[34] S. U. Khan and M. K. A. Rahim, "Correction of failure in antenna array using matrix pencil technique," *Chin. Phys. B*, vol. 26, no. 6, pp. 1–8, Jun. 2017.
[35] B. Appasani, R. Pelluri, and N. Gupta, "Detection and correction of errors in linear antenna arrays," *Int. J. Numer Model.*, vol. 31, pp. 1–12, Apr. 2018.
[36] S. U. Klhan, I. M. Qureshi, and B. Shoaib, "Recovery of failed element signal with a digitally beamforming using linear symmetrical array antenna," *J. Inf. Sci. Eng.*, vol. 32, no. 3, pp. 611–624, Mar. 2016.
[37] Z. Wang, C. Pang, Y. Li, and X. Wang, "A method for radiation pattern reconstruction of phased-array antenna," *IEEE Antennas Wireless Propag. Lett.*, vol. 19, no. 1, pp. 168–172, Jan. 2020, doi: 10.1109/LAWP.2019.2956761.
[38] H. Singh, H. L. Sneha, and R. M. Jha, "Mutual coupling in phased arrays: A review," *Int. J. Antennas Propag.*, vol. 2013, pp. 1–23, Mar. 2013.
[39] S. Lou, W. Wang, H. Bao, N. Hu, G. Ge, X. Hu, S. Qian, and C. Ge, "A compensation method for deformed array antennas considering mutual coupling effect," *IEEE Antennas Wireless Propag. Lett.*, vol. 17, no. 10, pp. 1900–1904, Oct. 2018.
[40] X. Wang, J. Li, W. Chen, M. Zhang, J. Chen, and A. Zhang, "The effect of mutual coupling on the performance of GNSS antenna arrays," *IEEE Access*, vol. 8, pp. 20480–20487, Jan. 2020.
[41] A. A. Manga, R. Gillard, R. Loison, I. L. Roy-Naneix, and C. Renard, "Experimental validation of a correcting coupling mechanism to extend the scanning range of narrowband phased array antennas," *IEEE Trans. Antennas Propag.*, vol. 68, no. 3, pp. 2078–2086, Mar. 2020.
[42] R. Long, J. Ouyang, F. Yang, W. Han, and L. Zhou, "Multi-element phased array calibration method by solving linear equations," *IEEE Trans. Antennas Propag.*, vol. 65, no. 6, pp. 2931–2939, Jun. 2017.
[43] C. O. Sanchez, D. Mange, S. Smith, and A. Tyrrell, "Embryonics: A bio-inspired cellular architecture with fault-tolerant properties," *Genet. Program. Evolvable Mach.*, vol. 1, no. 3, pp. 187–215, Sep. 2000.
[44] Z. Zhang, Y. Qiu, X. Yuan, R. Yao, Y. Chen, and Y. Wang, "A self-healing strategy with fault-cell reutilization of bio-inspired hardware," *Chin. J. Aeronaut.*, vol. 32, no. 7, pp. 1673–1683, Jul. 2019.

SAI ZHU received the M.S. and Ph.D. degrees from the Ordnance Engineering College, in 2011 and 2015, respectively. He is currently a Lecturer with Army Engineering University. His research interests include performance degradation analysis and fault prediction of electronic equipment, and bio-inspired self-repairing technology for phased array antennas.

CHUNHUI HAN received the M.S. and Ph.D. degrees from the Ordnance Engineering College, in 2004 and 2008, respectively. She is currently a Lecturer with Army Engineering University. Her research interests include performance degradation analysis and fault prediction of electronic equipment, and bio-inspired self-repairing technology.

YAFENG MENG received the M.S. and Ph.D. degrees from the Ordnance Engineering College, in 2001 and 2004, respectively. He is currently an Associate Professor with Army Engineering University. His research interests include automatic testing technology and fault diagnosis of electronic equipment.

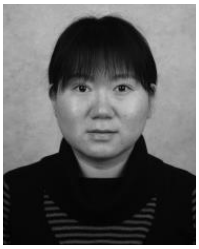

JIAWEN XU received the M.S. degree from Space Engineering University, in 2009. She is currently a Lecturer with Army Engineering University. Her research interests include fault prediction of electronic equipment and performance degradation analysis.

TING AN received the M.S. degree from North China Electric Power University, in 2015. She is currently a Lecturer with Army Engineering University. Her research interests include fault prediction of electronic equipment and antennas technology.